ASMS

CrossMark

RESEARCH ARTICLE

Optimizing Native Ion Mobility Q-TOF in Helium and Nitrogen for Very Fragile Noncovalent Structures

Valérie Gabelica,[1] Sandrine Livet,[1,2] Frédéric Rosu[3]

[1]Université de Bordeaux, CNRS, Inserm, Laboratoire Acides Nucléiques: Régulations Naturelle et Artificielle (ARNA, U1212, UMR5320), IECB, 2 rue Robert Escarpit, 33600, Pessac, France
[2]*Present Address:* CEA Saclay, DRF/JOLIOT, Service de Pharmacologie et d'Immunoanalyse, 91191, Gif sur Yvette Cedex, France
[3]Université de Bordeaux, CNRS, Inserm, Institut Européen de Chimie et Biologie (IECB, UMS3033, US001), 2 rue Robert Escarpit, 33600, Pessac, France
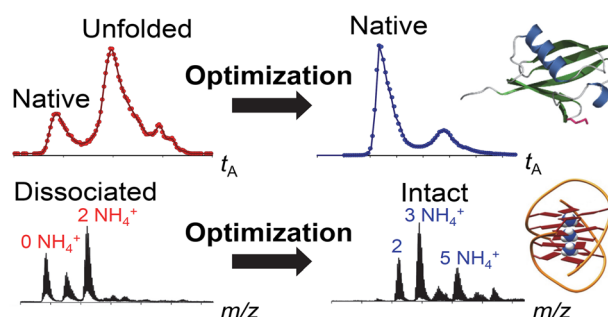
Abstract. The amount of internal energy imparted to the ions prior to the ion mobility cell influences the ion structure and thus the collision cross section. Non-covalent complexes with few internal degrees of freedom and/or high charge densities are particularly sensitive to collisional activation. Here, we investigated the effects of virtually all tuning parameters of the Agilent 6560 IM-Q-TOF on the arrival time distributions of ubiquitin[7+] and found conditions in which the native state prevails. We discuss the effects of solvent evaporation conditions in the source, of the entire pre-IM DC voltage gradient, of the funnel RF amplitudes. We also report on ubiquitin[7+] conformations in different solvents, including native supercharging conditions. Collision-induced unfolding (CIU) can be conveniently provoked either behind the source capillary or in the trapping funnel. The softness of the instrumental conditions behind the mobility cell was further optimized with the DNA G-quadruplex $[(dG_4T_4G_4)_2 \cdot (NH_4^+)_3 \text{-}8H]^{5-}$, for which ion activation results in ammonia loss. To reduce the ion internal energy and obtain the intact 3-NH_4^+ complex, we reduce the post-IM voltage gradient, but this results in a lower IM resolving power due to increased diffusion behind the drift tube. The article describes the various trade-offs between ion activation, ion transmission, and ion mobility performance for native MS of very fragile structures.

Keywords: Ion mobility, Native MS, Ion activation, Proteins, Nucleic acids

Introduction

Native mass spectrometry (native MS) involves measuring ions that have preserved a memory of the non-covalent interactions that were present in solution [1–4]. Intramolecular non-covalent interactions are responsible for the folding into specific secondary and tertiary structures, and intermolecular non-covalent interactions are responsible for the assembly of several molecules into complexes, also called "quaternary structures." The principles underlying native MS are common to mass spectrometry of intact biologically relevant molecules (proteins, nucleic acids, sugars) and of synthetic architectures [1] (artificial foldamers or supramolecular complexes). The main difference lies in the solution conditions in which the samples are dissolved for the analysis: biologically relevant complexes are studied in an electrospray-compatible buffer that best mimics the native cell environment in order to draw conclusions relevant to biology [5], whereas artificial architectures can be studied in any medium of interest.

The experimentalist should always ensure minimal perturbation of the non-covalent interactions to be detected in the gas phase so that the measurements provide information on the

Correspondence to: Valérie Gabelica; *e-mail:* v.gabelica@iecb.u–bordeaux.fr

structures that were originally present in the injected solution. For a mass analysis (detection of the complexes), this means that the intermolecular non-covalent interactions must be preserved from the source to the mass analyzer. For an ion mobility (IM) analysis (characterization of the shapes via the friction with a gas when dragged by an electric field [6, 7]), this means that the intramolecular non-covalent interactions must be preserved from the source to the mobility cell [8].

Here, we focused on the drift tube ion mobility instrument from Agilent (the 6560 IMS Q-TOF) [9], which like the Waters Vion IMS-QTof, the Tofwerk IMS-TOF, or the Bruker timsTOF has an ESI-IM-Q-TOF configuration (as opposed to the Waters Synapt™ instruments which have an ESI-Q-IM-TOF configuration). In this configuration, both rupture of intramolecular interactions before the IM cell and rupture of the intermolecular interactions between the IM cell and the mass analyzer can affect the interpretation of ion mobility results. Pre-IM activation causes a gas-phase unfolding that could be falsely attributed to a solution unfolding [10, 11]. Also, in IM calibration procedures, it is also extremely important that the calibrant ions are produced with the same distribution of collision cross sections in the calibrating instrument and in the calibrated instrument [12]. For this reason, native proteins were found to be poorer calibrants than denatured ones [13]. On the other hand, pre-IM activation can be exploited to study the gas-phase unfolding pathways, in so-called collision-induced unfolding (CIU) experiments [14], which are the IM analogue of collision-induced dissociation (CID) experiments in MS. Finally, post-IM fragmentation should often be avoided as well, because if the arrival time distribution of a given m/z range is actually the arrival time distribution of the parent ion that traveled in the IM and later led to the product ion having this particular m/z, IM could be misinterpreted.

The degree to which non-covalent interactions can be altered in the gas phase depends on the internal energy of the ions, on the number of degrees of freedom on which this internal energy is redistributed, on the number and strength of the interactions involved, and on the strength of Coulomb repulsion. Thus, complexes of smaller size and of higher charge density are more sensitive to ion activation. Here, we present how we optimized the Agilent 6560 IMS Q-TOF. We used bovine ubiquitin^{7+} to minimize pre-IMS unfolding and the DNA G-quadruplex $[(dG_4T_4G_4)_2 \cdot (NH_4^+)_3\text{-}8H]^{5-}$, which undergoes ammonia loss at low internal energy [15], to further minimize post-IMS fragmentation. Ubiquitin has frequently been used to assess IM instrument softness, because the IM profile of charge states 6+ to 8+ is extremely sensitive to internal energy effects, whether in the source [16], in the transfer [17], or in the pre-IM trapping region [18, 19]. The solution composition also plays a role on the detected gas-phase conformations [16, 20]. The native state of ubiquitin^{7+} has a collision cross section of ~ 1000 Å^2 in helium (~ 1300 Å^2 in nitrogen). In contrast with a recent report on the same instrument [21], we could obtain predominantly the native state on ubiquitin^{7+}, both in nitrogen and in helium drift tube conditions. For the G-quadruplex, we found that fragmentation mainly occurred after the IM when

using the default instrumental settings, and when lowering the voltage gradient, one had to trade-off softness for reduced IM resolution. We will describe here the rationale for optimizing the instrument for native MS of analytes bearing very fragile non-covalent interactions.

Experimental

Bovine ubiquitin, > 98% purity (SDS-PAGE), was purchased from Sigma (St Quentin Fallavier, France). The oligodeoxynucleotide strand dGGGGTTTTGGGG was purchased from Eurogentec (Seraing, Belgium). The G-quadruplex was prepared by mixing 100 µM single strands in 150 mM aqueous ammonium acetate, and waiting at least 24 h. Ammonium acetate 5 M solution (molecular biology grade) was from Fluka. Water was nuclease-free from Ambion™ (ThermoFischer Scientific, Illkirch, France). Acetic acid glacial, formic acid 99%, and methanol absolute were from Biosolve (Dieuze, France). Sulfolane 99% was from Aldrich (St Quentin Fallavier, France).

All experiments were run on an Agilent 6560 IMS-Q-TOF [9], equipped with the alternate gas kit, which regulates the drift tube pressure with a flow controller based on continuous readings with a capacitance gauge. The pumping system was modified in-house by using the default scroll pump for the rear of the instrument, and connecting an ECODRY 40 Plus pump (Leybold France SAS, Les Ulis, France) to the source region. To ensure appropriate pressure differentials for collision cross section determination, the pressures were set to 3.76 Torr in the drift tube and 3.47 Torr in the trapping funnel before the flow controller was turned on. This resulted, with the flow controller on, in pressures equal to 3.89 Torr in the drift tube and 3.63 Torr in the trapping funnel. The differential (0.26 Torr) ensures that only the intended gas (helium or nitrogen) is present in the drift tube, despite using atmospheric pressure ionization. The acquisition software version was B.07.00 build 7.00.7008. The IM data processing software IM-MS browser B.07.02 build 7.02.210.0 was used to calculate collision cross section values of well-defined peaks, and to export arrival time distributions. All graphs were constructed using SigmaPlot 12.5. For the CIU plots, because exported arrival time distributions may have too few data points in some regions, each arrival time distribution was smoothed using a negative exponential, sampling 0.02, and polynomial order 1, to produce evenly spaced data (200 intervals).

For ubiquitin in the positive mode, optimization of the pre-IMS zone was done on the 7+ ion with a 0.75 µM solution in 99% H$_2$O and 1% acetic acid, like in the Bleiholder group did for the soft tuning of trapped IMS [22]. Table 1 lists the parameter setpoints optimized by the manufacturer (on the Agilent tunemix ions) at the end of the installation of our instrument. We also list the parameters described by May et al. on their ubiquitin study, and the full list of parameters further optimized in the present study. The effects of changing each parameter will be described in the remainder of the paper.

Table 1. Tuning Parameters (Positive Mode) in the Pre-IMS Zone. All Voltages Are Floating on the Ion Mobility Tube Entrance. The Parameters Are Transposable to the Negative Mode by Reversing the Signs

Parameter	Installation by Agilent	May et al. [21]	Optimized on native Ubi^{7+}, drift tube in He	Optimized on native Ubi^{7+}, drift tube in N$_2$
Source: gas temperature	325 °C	25 °C	220 °C	220 °C
Source: drying gas	5.0 L/min	13 L/min	1.5 L/min	1.5 L/min
Source: nebulizer pressure	20 psig	None	9 psig	9 psig
Source: capillary	4000 V	Nanospray	3500 V	3500 V
Optics 1: fragmentor	400 V		300 V	300 V
IM front funnel: high pressure funnel delta	150 V		110 V	110 V
IM front funnel: high pressure funnel RF	150 V$_{p-p}$	80 V$_{p-p}$	100–180 V$_{p-p}$	100–180 V$_{p-p}$
IM front funnel: trap funnel delta	180 V		140 V	160 V
IM front funnel: trap funnel RF	150 V$_{p-p}$	80 V$_{p-p}$	160 V$_{p-p}$	100 V$_{p-p}$ for softness, 160 V$_{p-p}$ for CIU
IM front funnel: trap funnel exit	10 V		10 V	10 V
IM trap: trap entrance grid low	95 V		70 V	90 V
IM trap: trap entrance grid delta	10 V		2 V	2 V
IM trap: trap entrance	91 V		69 V	89 V
IM trap: trap exit	90 V		67 V	87 V
IM trap: trap exit grid 1 low	88 V		64 V	84 V
IM trap: trap exit grid 1 delta	6 V		5 V	5 V
IM trap: trap exit grid 2 low	87 V		63 V	83 V
IM trap: trap exit grid 2 delta	10 V		9 V	9 V
Acquisition: trap fill time	20,000 μs		1000 μs	1000 μs
Acquisition: trap release time	150 μs		200 μs	250 μs

To optimize the post-IMS zone for softness, we used the fragile bimolecular G-quadruplex [(dGGGGTTTT GGGG)$_2$·(NH$_4^+$)$_3$-8H]$^{5-}$ ion, which readily loses ammonia upon collisional activation [15]. It is the most collision-sensitive specific nucleic acid complex we know of, and frequently use it for instrument tuning [15]. The optimized pre-IMS parameters were first transposed to the negative mode from the ubiquitin optimized ones, by changing all signs. Then, the voltage gradients behind the IMS were lowered. MS/MS mode was off (collision energy = 0 V). Table 2 lists three sets of the various parameters that can be tuned: the default parameters at installation (which give the best transmission and mobility resolution), the parameters optimized for softness for the very fragile G-quadruplex, while still preserving most of the ion signal and a decent mobility separation (although with lower resolving power, see results and discussion), and a compromise that works for most moderately fragile complexes. Further examples are given in the results and discussion.

Results and Discussion

Tuning is a multiparametric and iterative process. To improve softness, the general reasoning is to reduce the ion acceleration by electric fields to reduce the laboratory frame collision energy between the ion and the background gas. However, there is often a compromise between softness and ion transmission. Also, too much softness can mean insufficient desolvation or declustering. Finally, the actual effect of a given voltage difference depends on the gas pressure and flows [23, 24]. We will show the effect of each type of parameter either side of our final optimized values to illustrate what happens when departing from this optimum. It must be understood, however, that there may exist different sets of parameter which could constitute another

optimum. We do not claim we have reached the global optimum, but we have reached one that suits our applications on native MS of ~ 10 kDa complexes and very fragile complexes, including for performing collision-induced unfolding experiments.

Tuning the Instrument Pre-IM Region for Softness

In the pre-IM region, we examined 20 different parameters. Figure 1 depicts the optimized DC voltage gradient from the end of the glass capillary to the IM entrance. Supporting information Fig. S1 compares visually the DC gradient in the default instrument tuning (which we presume is similar to that used by May et al. [21] unless otherwise specified in Table 1) and in the optimized tuning for the drift tube operated in helium. As detailed below, the main difference lies in the voltage gradients in the ion trapping region.

The voltage called "fragmentor," applied at the end of the glass capillary, was already known to influence softness. However, the tuning of the other parameters was less intuitive, and we found one voltage difference (between the trap entrance and the trap entrance grid) that unexpectedly had a large influence on the results. All parameters are explained in detail below. We focus here on describing the tuning for softness with the drift tube in helium, which was more sensitive than in nitrogen, and will mention any differences found in nitrogen.

DC Level of the Trapping Region All DC voltages are floating on the IM entrance, which is thus defined here as 0 V. The trapping funnel is located before the IM entrance. The trapping funnel has an hourglass shape, with an entrance, an exit, and the trapping region delimited by grids. Further towards the

Table 2. Tuning Parameters (Negative Mode) in the Post-IMS Region. The "Optimized" and "Compromise" Parameters Are Transposable to the Positive Mode by Reversing the Signs

Parameter	Installation by Agilent, suitable for intramolecular folding studies	Compromise for moderately fragile noncovalent complexes	Optimized on very fragile G-quadruplex
IM drift tube: drift tube exit	− 250 V	− 210 V	− 210 V
IM rear funnel: rear funnel entrance	− 240 V	− 200 V	− 200 V
IM rear funnel: rear funnel RF	150 V_{p-p}	180 V_{p-p}	180 V_{p-p}
IM rear funnel: rear funnel exit	− 43 V	− 35 V	− 26 V
IM rear funnel: IM Hex Entrance	− 41 V	− 32 V	− 24 V
IM rear funnel: IM Hex Delta	− 9 V	− 3 V	− 2 V
Optics 1: Oct Entrance Lens	− 32 V	− 27 V	− 21 V
Optics 1: Oct 1 DC	− 31.3 V	− 25 V	− 20 V
Optics 1: Lens 1	− 29.4 V	− 23 V	− 19 V
Optics 1: Lens 2	Disabled	Disabled	Disabled
Quad: Quad DC	− 27.8 V	− 21 V	− 18 V
Quad: postfilter DC	− 27.8 V	− 21 V	− 17 V
Cell: gas flow	22 psi	20 psi	20 psi
Cell: cell entrance	− 26.8 V	− 20 V	− 16 V
Cell: Hex DC	− 25.8 V	− 20 V	− 16 V
Cell: Hex Delta	9 V	3 V	3 V
Cell: Hex2 DC	− 16.6 V	− 14.6 V	− 12 V
Cell: Hex2 DV	3 V	1.5 V	1 V
Optics 2: Hex3 DC	− 13.2 V	− 12.9 V	− 11 V
Extractor: ion focus	− 10 V	− 10 V	− 10 V

source, we find the high pressure funnel (which has entrance and exit voltages), and the "fragmentor", which accelerates ions from the glass capillary towards the HP funnel. As shown in Fig. 1 and Table 1, on the data acquisition software for some voltages, one enters absolute values, and for others, one enters voltages differences ("delta"s). The trap funnel exit is optimum at 10 V in all cases. The voltage levels of the trapping region of the trapping funnel (in the 70-V range on Fig. 1) will influence the acceleration energy of ions released from the trap and injected in the drift tube.

In Fig. 2a, we show that this "injection energy" influences the softness. In helium, when the trap DC voltages are in the 90- or 100-V range, such as in typical installation parameters for nitrogen, the conditions are less soft and the peak of the native conformation at ∼ 25 ms disappears to the profit of more extended (longer drift time) conformations. Too low trap DC voltages are also detrimental, because the IM peaks are shifted to longer times. The reason is that the ions travel slower to the IM: This delay contributes to the dead time t_0 (time spent outside the drift region), and the
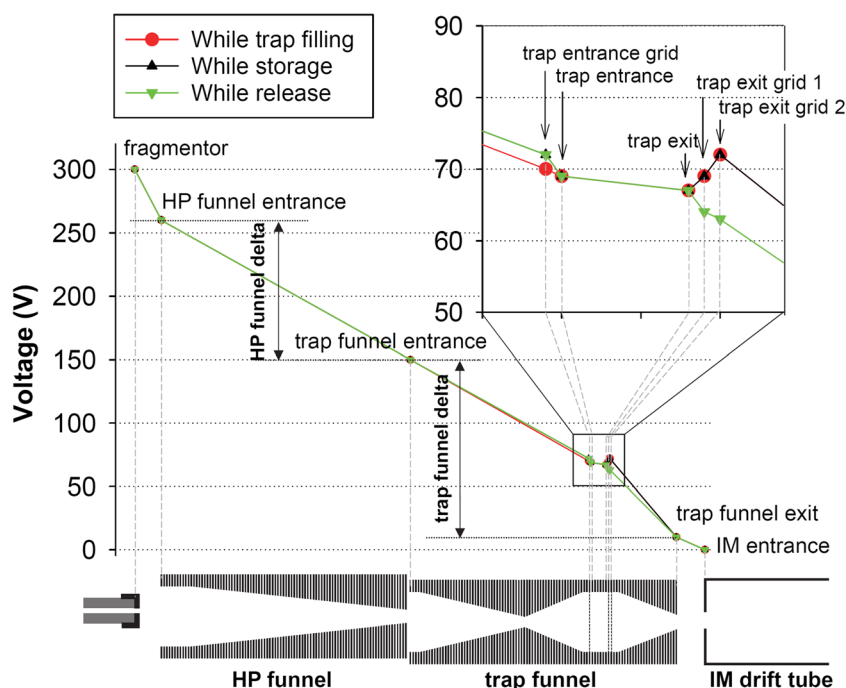
Figure 1. DC voltage profile before the ion mobility (IM) drift tube entrance, with parameters optimized for 3.89 Torr helium in the drift tube and a pressure differential of 0.26 Torr compared to the trapping funnel. The parameters are listed in Table 1
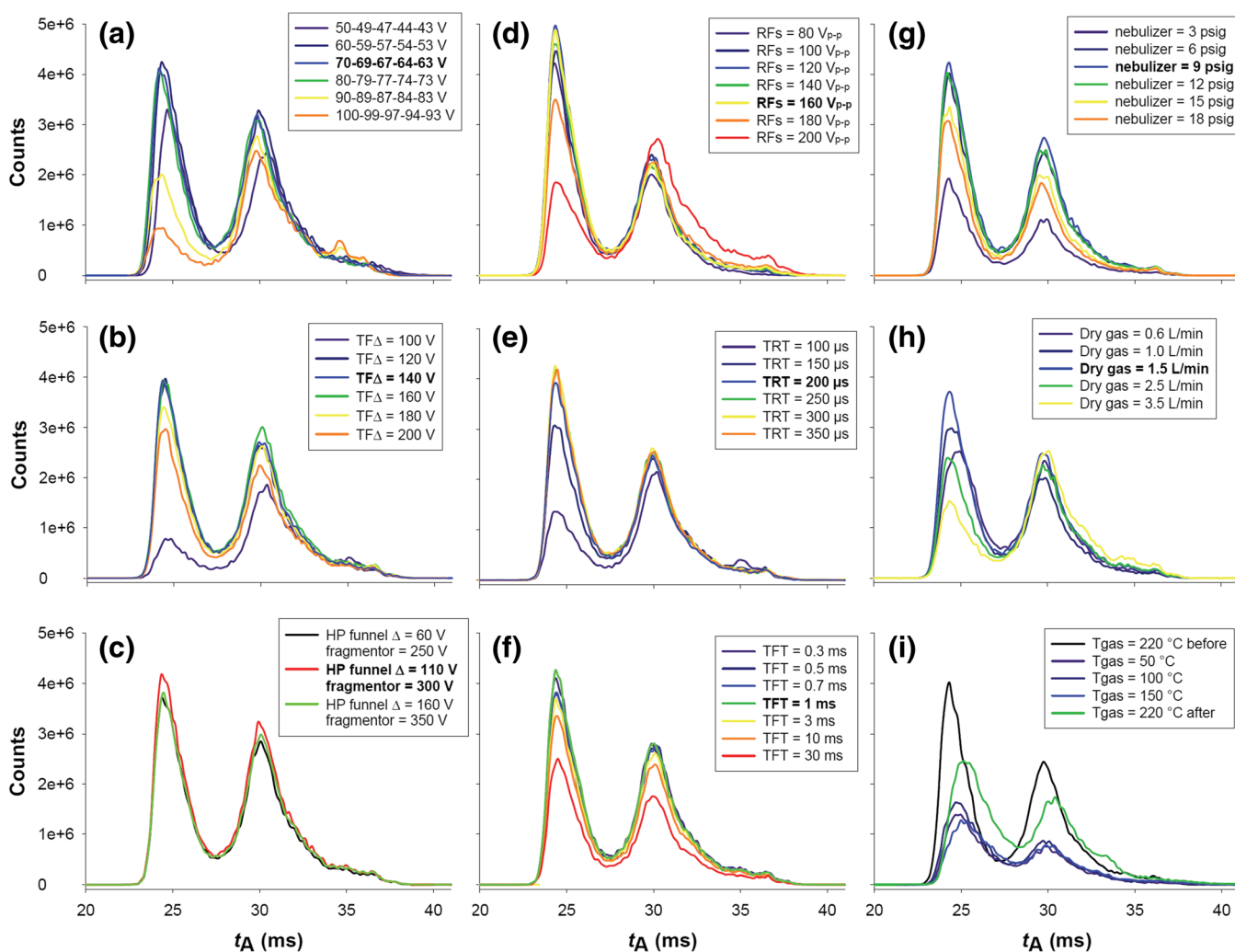
Figure 2. Influence of various tuning parameters on the arrival time distribution of Ubiquitin[7+], sprayed from a 0.75 µM solution in 99% H_2O and 1% acetic acid, with the drift tube operated in 3.89 Torr helium. The same number of scans were summed in all cases. The drift tube was operated with $\Delta V = 390$ V. The peak at ~ 25 ms corresponds to the native form ($CCS_{He} = 981$ Å^2; standard deviation was 7 Å^2 from 10 independent measurements). The optimum value is in bold. Effects of (**a**) voltages on the whole trapping region (see inset of Fig. 1), the values written being the trap entrance grid low-trap entrance-trap exit-trap exit grid 1 low-trap exit grid 2 low; (**b**) trap funnel delta; (**c**) HP funnel RF and front funnel RF, both set at the same value; (**d**) trap release time; (**e**) trap fill time; (**f**) HP funnel delta and fragmentor voltage; (**g**) electrospray nebulizer pressure; (**h**) dry gas flow; and (**i**) dry gas temperature effect, in order of recording. Note that after lowering the temperatures for a while, the system takes a very long time to recover its initial condition

conditions are detrimental to the resolving power. In helium, the optimum trap DC level is thus in the 70-V range. In nitrogen, the activation effects are less acute (see supporting Fig. S2A), and the 90-V range is optimum, because in the 70-V range, the ions drift too slowly towards the IM. The influence of other voltages in the trapping region will be discussed in the section on CIU. The parameters listed in Table 1 are the softest ones that do not compromise ion trapping efficiency or IM resolution.

Funnel DC Gradients Continuing towards the source, we have the trap funnel entrance, which voltage is equal to the trap funnel exit voltage plus the trap funnel delta. Figure 2b

shows the influence of the trap funnel delta. At high values (200 V is the maximum allowed), the conditions become slightly activating, and one loses signal intensity. But counter-intuitively, at low voltages (100 V), the conditions are also more activating, and the signal is lower. A possible explanation is that if the ions move too slowly between the funnel entrance through the hourglass to the trapping region, they wander around longer before entering in the trapping region and thus have time to be activated by the RF and change conformation. Our results therefore suggest that ion trapping in the first part of the funnel can occur at too low voltages. The optimum front funnel delta voltage was set to 140 V in helium (160 V in nitrogen, in line with the trap level which is also 20 V higher, see Fig. S2B). In contrast, the high-pressure funnel

delta shows no such effects, and any value of HP funnel delta between 60 and 160 V gives similar results (Fig. 2c). A possible explanation is that the gas flows play a larger role than the voltage gradient on the ion transport in this region, and thus trapping does not occur. The fragmentor voltage defines an acceleration region at the entrance of the high-pressure funnel, and its effect will be described in the section on CIU. For soft conditions, its value is set slightly above the HP funnel entrance absolute value.

Trapping Funnel RF Amplitude　The high-pressure funnel and trap funnel have also radiofrequencies (1.5 MHz for the high-pressure funnel, 1.2 MHz for the trapping funnel). May et al. described that both RF amplitudes must be decreased to 80 V_{p-p} to have softer conditions. We reproduced this trend when operating the drift tube in nitrogen (Fig. S2C), and chose 100 V_{p-p} to optimize the signal. However, in helium, the situation is different: from 80 to 160 V_{p-p}, no significant ion activation was observed. Unfolding is only noticed at 180 V_{p-p} and higher (in nitrogen, unfolding is noticeable already at 140 V_{p-p}). The reason for the difference is that when helium is used in the IM tube, helium is also injected in the funnels to avoid nitrogen contamination in the tube, and ions move faster overall. Thus, in helium, similar RF amplitudes have a lower effect on ion activation than in nitrogen.

It is surprising that the trap funnel RF amplitude has a greater effect on ion activation in nitrogen than in helium, while the DC gradients in the same region have a greater effect in helium than in nitrogen. A possible origin of the difference could be a different positioning of the ion cloud in the trapping region, depending on the ion gas, for given RF amplitudes. If radial ion placement differs according to the gas composition, it is possible that a given DC voltage difference has different effects for the ions in terms of actual electric field. However, to test whether this hypothesis explains the observations, simulations of ion trajectories in the presence of collisions with the background gases would be required.

We will describe below that it is possible to carry out CIU experiments in the trapping region. To do that, however, the trap funnel RF amplitude has to be high enough, presumably to confine the ions in the region where the DC gradient is applied. Also, for larger ions, the RF amplitudes have to be increased (for example, 200 V_{p-p} is optimum for native bovine serum albumin (66 kDa) transmission, data not shown). The final choice of the RF amplitudes will thus depend on the type of experiment: 100 V_{p-p} for native MS on fragile molecules in nitrogen, and 160 V_{p-p} or higher in helium and for CIU. We also found that the HP funnel RF amplitude had no effect on transmission and softness (Fig. S3): 100 and 180 V_{p-p} give the same results. Again, gas flows may dictate ion transport more than voltages in the high-pressure funnel.

Trapping and Release Times　We noticed an effect of the trap release time (the time during which the trap voltages are set to the green ramp in Fig. 1, to push the ions towards the IM) on the arrival time distribution. Short trap release times are supposed to help bunch the ion packet towards the IM with a short time spread (contributing minimally to the width of t_0). However, with trap release times shorter than 200 μs, ubiquitin gets more activated and the total ion signal decreases (Fig. 2e). A possible explanation is that the fraction of the ion population that had the opportunity to exit the trap during short release times had to do so quickly and thus traveled faster and got activated more. Longer times than 200 μs did not change the allure of the peaks. The same effect was observed in nitrogen, and the optimum for softness was 250 μs. Again, the difference comes from the slower movement of ions in nitrogen.

The trap fill time (Fig. 2f) did not influence the softness. However, the ion signal decreases at long trap fill times. Normally, the ion signal should increase linearly with the fill time unless there is space charge, as described on a similar trap with one entrance grid and two exit grids [25]. The same phenomenon was observed on a solution 10 times less concentrated (0.075 μM, see Fig. S4), giving 10 times lower signal with the standard ESI source, so the phenomenon is not due to space charge. The origin of this phenomenon is unknown.

Influence of the Electrospray Source Parameters

We also examined how the electrospray source parameters influence the activation of ubiquitin[7+]. Here, the effects of the electrospray process (at stake in the intermediate phase consisting of the dense solvent plume) and of ion activation (desolvated ions undergoing collisions) may be combined. The nebulizer gas flow had no effect on the apparent activation. It had only an effect on the ion signal and the optimum was at 9 psig. This parameter should be optimized based on ion signal for each solvent.

In contrast, the drying gas flow influences the apparent ion activation. In the standard electrospray source, a heated drying gas is coming from the entrance capillary, countercurrent to the spray. At 220 °C, high flows cause substantial activation, and low flows resulted in lower ion signals. The optimum drying gas flow, for ubiquitin infused at 190 μL/h, was 1.5 L/min.

The drying gas temperature, when decreased, also resulted in decreased ion signals, without necessarily decreasing the apparent ion activation. The droplets interact only very transiently with the heated nebulizer gas and undergo endothermic evaporation. Consequently, the effect of gas heating is not equivalent to heating the solution, and gas temperatures higher than the solution melting temperature can be used. However, too low temperatures were very detrimental to the IM signals: Over a time scale of several minutes, the IM peaks started to shift to longer drift times, and even when going back to the usual temperature of 220 °C, the shift persisted for over an hour. Our interpretation is that when the drying gas temperature is too low, significant amounts of electrospray solvent enter the funnels and eventually contaminate the drift tube, where even trace amounts of polar molecules in the helium bath gas slow

down the ions. Given that the drying gas temperature did not affect the apparent harshness of the conditions, we recommend using sufficiently high temperatures in electrospray, to avoid solvent contamination in the pressure differential. We found that solvent-dependent contamination problems in the tube are more likely to occur when the drift tube is operated in helium, compared to nitrogen.

Finally, we compared three different ion sources: the standard ESI source (results above), the JetStream™ source (Agilent Technologies), and static nanospray ionization using extra coated L borosilicate capillaries (ThermoFischer Scientific, Illkirch, France). Figure S5 shows the comparison for ubiquitin^{7+}, with nitrogen as drift gas. The standard ESI source appears slightly softer. Similar conclusions were reached by Konermann's group on a Waters Synapt ion mobility mass spectrometer [13].

Comparison of Ubiquitin Sprayed from Different Solvents

To compare ubiquitin sprayed from different solvents, we thus used the drift tube in nitrogen. After starting the injection of each solvent mixture for at least 5 min, we controlled the pressure differential with the flow controller off then on again, and then recorded the data presented here. The optimum source and transfer conditions of Table 1 were used for all solvent mixtures. The resulting arrival time distributions are shown in Fig. 3.

Figure 3a shows the arrival time distribution obtained in water/methanol and 0.2% formic acid, i.e., the denaturing conditions used by May et al. on the Agilent 6560 [21]. Even with the optimized soft instrument tuning, the conformations under this charge state are mostly denatured. In contrast, when using 1% acetic acid instead of 0.2% formic acid (Fig. 3b), which are the conditions used by Russell's group on the Waters Synapt [26], despite that the charge state distribution is also centered on high charge states, the conformations under the 7+ charge state are predominantly compact, which may be due to a small fraction still having a native fold in solution. The apparent discrepancy between the results of May et al. and Russell et al. was thus mainly due to the solvent choice.

In the interest of native MS, we also investigated native supercharging conditions, here 0.5% sulfolane in 150 mM NH$_4$OAc (Fig. 3c). The 7+ ion is abundant and its arrival time distribution is mainly constituted from a compact conformation, and the conditions appear even softer than in H$_2$O/acetic acid (Fig. 3f). However, the peak is slightly offset to a higher collision cross section (1337 Å^2) compared to all sample preparations without sulfolane (1262 Å^2, standard deviation 9 Å^2 from $N = 6$ experiments). In comparison, the compact peak obtained from 50 mM NH$_4$OAc (i.e., Russell's native conditions [26], Fig. 3d) or 20 mM NH$_4$OAc (i.e., May's native conditions [21], Fig. 3e) is similar to the one obtained from aqueous acetic acid (Fig. 3f). The supercharging mechanisms in the presence of
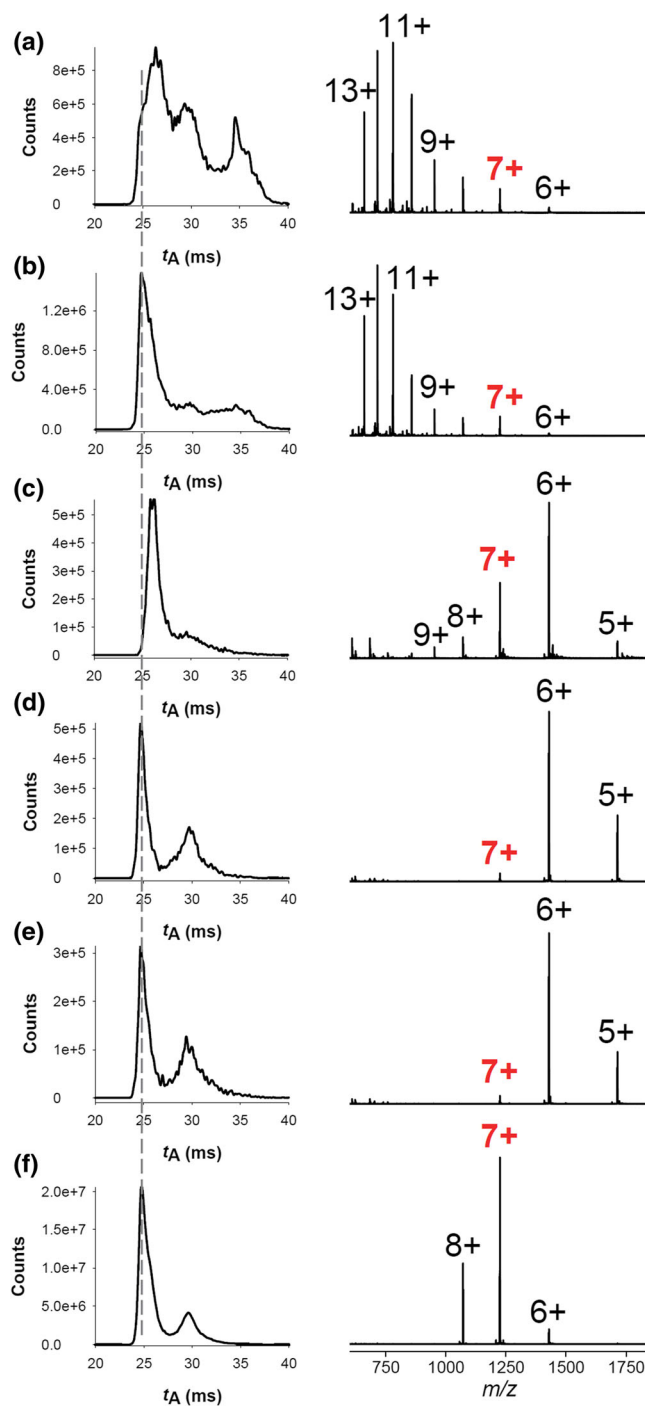

Figure 3. Arrival time distribution of the ubiquitin^{7+} and charge state distributions obtained from different solvents (drift tube in 3.89 Torr nitrogen, $\Delta V = 1390$ V). (a) H$_2$O/MeOH/formic acid (49.9/49.9/0.2% vol). (b) H$_2$O/MeOH/acetic acid (49.5/49.5/1% vol). (c) 150 mM NH$_4$OAc, 0.5% sulfolane. (d) 50 mM NH$_4$OAc. (e) 20 mM NH$_4$OAc. (f) H$_2$O/acetic acid (99/1% vol)

NH$_4$OAc are still a subject of debate [27–30], and our results suggest that although the conformations are compact, they are not necessarily identical to the native ones. These preliminary results call for further systematic studies, which are beyond the scope of this paper and will be reported elsewhere.
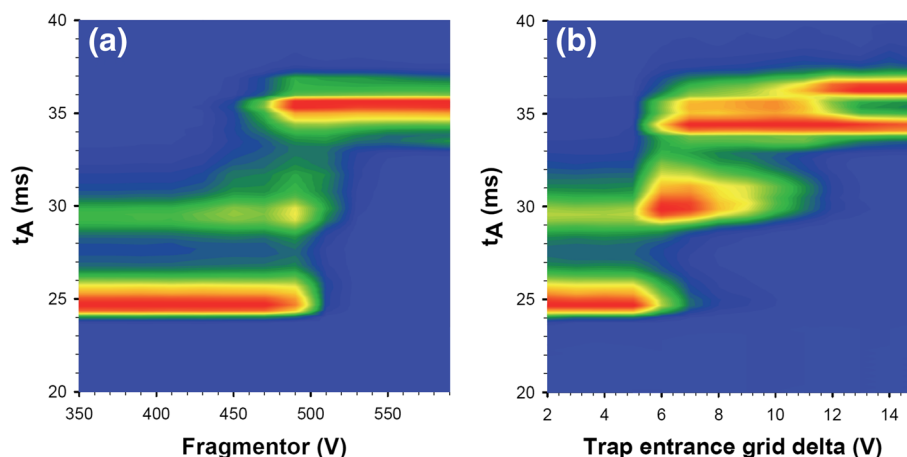
Figure 4. Collision-induced unfolding (CIU) of ubiqutin^{7+}, with the drift tube in 3.89 Torr nitrogen (optimized voltages from Table 1, $\Delta V = 1390$ V), obtained by changing (**a**) the fragmentor voltage (trap funnel RF amplitude = 100 V$_{p-p}$) or (**b**) the trap entrance grid delta voltage (trap funnel RF amplitude = 160 V$_{p-p}$)

Collision-Induced Unfolding (CIU) Experiments

We found two parameters that could cause substantial activation: the fragmentor voltage and the trap entrance grid delta. The fragmentor is accelerating the ions between the extremity of the coated glass capillary and the entrance of the high-pressure funnel. Figure 4a shows the resulting CIU plot: At 450 V, the abundance of the intermediate state becomes slightly larger, and at 490 V, an extended state appears.

Figure 4b shows that CIU plots can also be obtained by varying the trap entrance grid delta, which is the voltage difference between the trap entrance grid "low" (during trap filling) and "high" (during storage and release, see Fig. 1). This means that, after filling, the ions in the trap are subjected, on the entrance side, to a sudden voltage difference equal to (trap entrance grid delta + trap entrance grid low − trap entrance), and that this voltage can activate the entire ubiquitin^{7+} population to unfold it. Note that for carrying out CIU experiments using the trap entrance grid delta voltage, the trap funnel RF amplitude has to be increased to 160 V$_{p-p}$. Too low trap RF amplitudes result in signal losses at some voltages, and aberrant CIU plots if normalization is done spectrum per spectrum (see Fig. S6).

Comparing Fig. 4a, b also reveals that the activation processes are not equivalent in the two regions. When ubiquitin^{7+} is activated in the trap, three distinct extended conformations are produced, eventually two at the highest voltages. This is in line with previous reports by IMS-IMS [17, 20], CIU in a Waters Synapt [31], and by activated TIMS [32]. When activated in the fragmentor region, however, a single extended population is observed, which is broader and at a median arrival time compared to the conformers found by activation in the trap. We conjecture that residual solvent vapor may still be present in the high-pressure funnel where the fragmentor operates and that ion-molecule reactions could contribute rearranging the extended conformers. This hypothesis would warrant further investigation, depending on source conditions and on the solvent, and if confirmed, comparing CIU in the fragmentor and in the trap could be a useful method to compare CIU in partially solvated vs. gas phase environments.

Optimization of the Post-IM Region for Fragile Non-covalent Complexes

When fragmentation of very fragile complexes must be reduced also behind the drift tube, the voltage gradients from the rear funnel down to the TOF region can be lowered. After choosing the softest parameters before the IM, we optimized the post-IM region using the ammonium-bound bimolecular G-quadruplex [(dGGGGTTTT GGGG)$_2$·(NH$_4^+$)$_3$-8H]$^{5-}$, which served to benchmark several instruments [15], and the results are shown in Fig. 5. In addition to the default parameters provided by the manufacturer following installation, we devised two sets of voltage gradients: one is the softest that is still compatible with IMS for our complexes, while minimizing fragmentation ("very fragile" tuning parameters), and one is a compromise giving higher transmission and better IM resolution. The voltage gradients are shown in Fig. 5a. Again, some of the applied voltages are differences between an entrance and a delta voltage entered in the data acquisition software. By lowering the entire voltage gradient, we could obtain the intact three-ammonium complex as the major species when the drift tube is in helium (Fig. 5d), and even the five-ammonium complex, which is also specific [15], with the drift tube in nitrogen (Fig. 5g).

The choice of the voltage set depends on the application. If post-IM fragmentation is to be avoided at all costs, the shallowest possible gradient is recommended, but this comes at the expense of ion signal and IM resolution, as shown in Fig. S7 on ubiquitin^{7+}. With too shallow gradients, the ions wander around longer, so the time spent
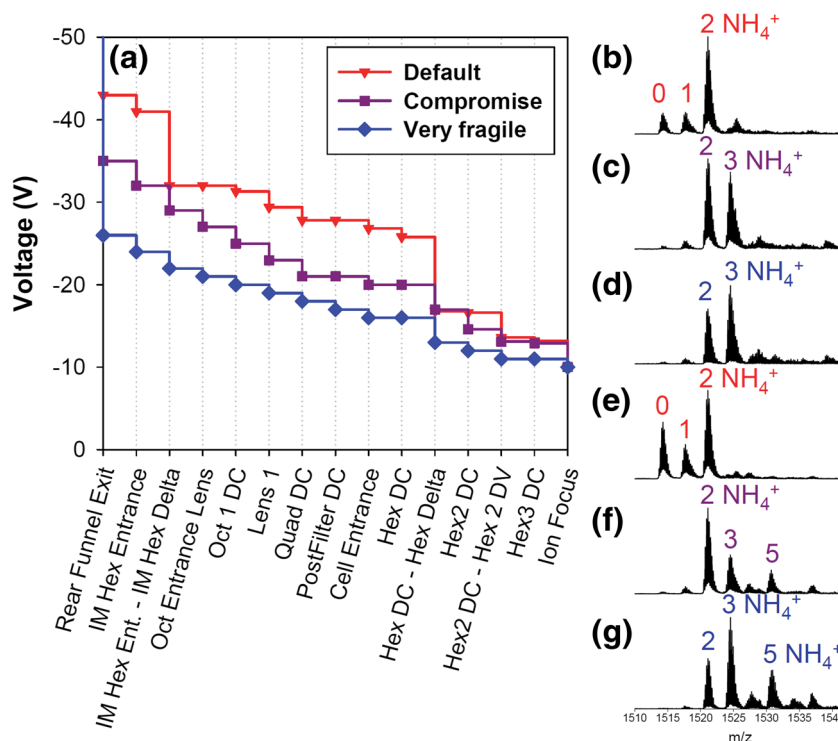
Figure 5. (a) Illustration of the DC voltage gradient behind the drift tube in negative mode, with the three sets of voltages listed in Table 2. (b–g) ammonium adduct distribution on the bimolecular G-quadruplex $[(dG_4T_4G_4)_2 \cdot (NH_4^+)_n - (5+n)H^+]^{5-}$, obtained in helium (b–d) with the three different gradients ((b) default, (c) compromise, (d) very fragile) and in nitrogen (e–g, same color code)

outside the IM drift tube (t_0) increases, and diffusion increases. With extremely shallow gradients, one may even reach a limit where the ions are trapped in hexapoles, and all IM resolution is lost (MS analysis is still feasible). For studying purely intramolecular conformations (provided that no multimer dissociation is interfering), the default steeper gradients should be used, to maintain the best possible IM resolution.

Conclusions

Optimizing the Agilent IMS-Q-TOF for native MS, especially when the drift tube is operated in helium, required departing significantly from the recommended default settings. After examining systematically the combined effects of nearly 40 parameters, we obtained conditions allowing to obtain mainly the native ubiquitin^{7+} conformation, and the intact fragile G-quadruplex [(dGGGGTTTT GGGG)$_2$·(NH$_4^+$)$_3$-8H]$^{5-}$. The main difference between our IM profiles and those reported by May et al. [21] come from (i) the solvent used and (ii) ion release conditions from the trap to the IM. The voltage difference between the trap entrance grid and the trap entrance is a key parameter to tune ion activation in the trapping region.

Some tuning parameters differ in helium and in nitrogen because the ions move faster in helium, and slightly softer

conditions could be obtained in nitrogen. We also demonstrated that collision-induced unfolding (CIU) experiments could be conducted in two different ways: by increasing the fragmentor voltage or by increasing the trap entrance grid delta voltage. Both types of CIU data are interesting, given that the fragmentor operates in a region where solvent vapors may still be present, whereas the trapping region is closer to pure gas-phase conditions.

Understanding all these parameters will be useful for several kinds of native MS applications, for example to choose conditions that minimally perturb the structures coming from the solution, to activate them intentionally, or to minimize fragmentation both before and after the IM in order to correctly assign the mobility peaks. In future work, the optimized tuning described herein can be exploited to investigate particularly fragile complexes, for example maintained by only a few weak non-covalent interactions, or with high charge densities and thus higher Coulomb repulsion between subunits.

Funding Information

References

1. Schalley, C.A.: Supramolecular chemistry goes gas phase: the mass spectrometric examination of non-covalent interactions in host-guest chemistry and molecular recognition. Int. J. Mass Spectrom. **194**, 11 (2000)

2. Loo, J.A.: Studying non-covalent protein complexes by electrospray ionization mass spectrometry. Mass Spectrom. Rev. **16**, 1 (1997)

3. Smith, R.D., Light-Wahl, K.J.: The observation of non-covalent interactions in solution by electrospray ionization mass spectrometry: promise, pitfalls and prognosis. Biol. Mass Spectrom. **22**, 493 (1993)

4. Schalley, C.A., Springer, A.: Mass Spectrometry and Gas-Phase Chemistry of Non-Covalent Complexes. Wiley, Hoboken (2009)

5. Leney, A.C., Heck, A.J.R.: Native mass spectrometry: what is in the name? J. Am. Soc. Mass Spectrom. **28**, 5 (2017)

6. Kanu, A.B., Dwivedi, P., Tam, M., Matz, L., Hill, H.H.: Ion mobility-mass spectrometry. J. Mass Spectrom. **43**, 1 (2008)

7. Clemmer, D.E., Jarrold, M.F.: Ion mobility measurements and their applications to clusters of biomolecules. J. Mass Spectrom. **32**, 577 (1997)

8. Wyttenbach, T., Bowers, M.T.: Intermolecular interactions in biomolecular systems examined by mass spectrometry. Annu. Rev. Phys. Chem. **58**, 511 (2007)

9. May, J.C., Goodwin, C.R., Lareau, N.M., Leaptrot, K.L., Morris, C.B., Kurulugama, R.T., Mordehai, A., Klein, C., Barry, W., Darland, E., Overney, G., Imatani, K., Stafford, G.C., Fjeldsted, J.C., McLean, J.A.: Conformational ordering of biomolecules in the gas phase: nitrogen collision cross sections measured on a prototype high resolution drift tube ion mobility-mass spectrometer. Anal. Chem. **86**, 2107 (2014)

10. Gabelica, V., Marklund, E.: Fundamentals of ion mobility spectrometry. Curr. Opin. Chem. Biol. **42**, 51 (2018)

11. Clemmer, D.E., Russell, D.H., Williams, E.R.: Characterizing the Conformationome: toward a structural understanding of the proteome. Acc. Chem. Res. **50**, 556 (2017)

12. Bush, M.F., Hall, Z., Giles, K., Hoyes, J., Robinson, C.V., Ruotolo, B.T.: Collision cross sections of proteins and their complexes: a calibration framework and database for gas-phase structural biology. Anal. Chem. **82**, 9557 (2010)

13. Sun, Y., Vahidi, S., Sowole, M.A., Konermann, L.: Protein structural studies by traveling wave ion mobility spectrometry: a critical look at electrospray sources and calibration issues. J. Am. Soc. Mass Spectrom. **27**, 31 (2016)

14. Zhong, Y., Han, L., Ruotolo, B.T.: Collisional and coulombic unfolding of gas-phase proteins: high correlation to their domain structures in solution. Angew. Chem. Int. Ed. **53**, 9209 (2014)

15. Balthasart, F., Plavec, J., Gabelica, V.: Ammonium ion binding to DNA G-quadruplexes: do electrospray mass spectra faithfully reflect the solution-phase species? J. Am. Soc. Mass Spectrom. **24**, 1 (2013)

16. Li, J., Taraszka, J.A., Counterman, A.E., Clemmer, D.E.: Influence of solvent composition and capillary temperature on the conformations of electrosprayed ions: unfolding of compact ubiquitin conformers from pseudonative and denatured solutions. Int. J. Mass Spectrom. **185/186/187**, 37 (1999)

17. Koeniger, S.L., Merenbloom, S.I., Sevugarajan, S., Clemmer, D.E.: Transfer of structural elements from compact to extended states in unsolvated ubiquitin. J. Am. Chem. Soc. **128**, 11713 (2006)

18. Myung, S., Badman, E.R., Lee, Y.J., Clemmer, D.E.: Structural transitions of electrosprayed ubiquitin ions stored in an ion trap over ~10 ms to 30 s. J. Phys. Chem. A. **106**, 9976 (2002)

19. Wyttenbach, T., Bowers, M.T.: Structural stability from solution to the gas phase: native solution structure of ubiquitin survives analysis in a solvent-free ion mobility-mass spectrometry environment. J. Phys. Chem. B. **115**, 12266 (2011)

20. Shi, H., Atlasevich, N., Merenbloom, S.I., Clemmer, D.E.: Solution dependence of the collisional activation of ubiquitin [M + 7H](7+) ions. J. Am. Soc. Mass Spectrom. **25**, 2000 (2014)

21. May, J.C., Jurneczko, E., Stow, S.M., Kratochvil, I., Kalkhof, S., McLean, J.A.: Conformational landscapes of ubiquitin, cytochrome c, and myoglobin: uniform field ion mobility measurements in helium and nitrogen drift gas. Int. J. Mass Spectrom. **427**, 79 (2018)

22. Liu, F.C., Kirk, S.R., Bleiholder, C.: On the structural denaturation of biological analytes in trapped ion mobility spectrometry - mass spectrometry. Analyst. **141**, 3722 (2016)

23. Schmidt, A., Bahr, U., Karas, M.: Influence of pressure in the first pumping stage on analyte desolvation and fragmentation in nano-ESI MS. Anal. Chem. **73**, 6040 (2001)

24. Gabelica, V., De Pauw, E.: Internal energy and fragmentation of ions produced in electrospray sources. Mass Spectrom. Rev. **24**, 566 (2005)

25. Clowers, B.H., Ibrahim, Y.M., Prior, D.C., Danielson III, W.F., Belov, M.E., Smith, R.D.: Enhanced ion utilization efficiency using an electrodynamic ion funnel trap as an injection mechanism for ion mobility spectrometry. Anal. Chem. **80**, 612 (2008)

26. Chen, S.H., Russell, D.H.: How closely related are conformations of protein ions sampled by IM-MS to native solution structures? J. Am. Soc. Mass Spectrom. **26**, 1433 (2015)

27. Hogan Jr., C.J., Ogorzalek Loo, R.R., Loo, J.A., de la Mora, J.F.: Ion mobility-mass spectrometry of phosphorylase B ions generated with supercharging reagents but in charge-reducing buffer. Phys. Chem. Chem. Phys. **12**, 13476 (2010)

28. Sterling, H.J., Kintzer, A.F., Feld, G.K., Cassou, C.A., Krantz, B.A., Williams, E.R.: Supercharging protein complexes from aqueous solution disrupts their native conformations. J. Am. Soc. Mass Spectrom. **23**, 191 (2012)

29. Chingin, K., Xu, N., Chen, H.: Soft supercharging of biomolecular ions in electrospray ionization mass spectrometry. J. Am. Soc. Mass Spectrom. **25**, 928 (2014)

30. Ogorzalek Loo, R.R., Lakshmanan, R., Loo, J.A.: What protein charging (and supercharging) reveal about the mechanism of electrospray ionization. J. Am. Soc. Mass Spectrom. **25**, 1675 (2014)

31. Wagner, N.D., Kim, D., Russell, D.H.: Increasing ubiquitin ion resistance to unfolding in the gas phase using chloride adduction: preserving more "native-like" conformations despite collisional activation. Anal. Chem. **88**, 5934 (2016)

32. Ridgeway, M.E., Silveira, J.A., Meier, J.E., Park, M.A.: Microheterogeneity within conformational states of ubiquitin revealed by high resolution trapped ion mobility spectrometry. Analyst. **140**, 6964 (2015)